MECHANICAL FAILURE OF A COMPOSITE HELICOPTER STRUCTURE UNDER STATIC LOADING

Steven Roy, Larry Lessard

Dept. of Mechanical Engineering, McGill University, Montreal, Québec, Canada

ABSTRACT

The design and mechanical performance of a helicopter horizontal stabilizer slat made by RTM can be evaluated with finite element analysis. However, uncertainties arise from the assumptions used for simplifying the model in the analysis, especially when the materials are anisotropic, inhomogeneous and can present defects originating from the manufacturing process.

To verify the validity of the assumptions used in the modeling of the slat structure, static mechanical tests are performed on prototype slats which are one third of the full-size length. The slat complex boundary conditions were simplified to make static mechanical testing possible. A fixture was designed to introduce the simplified loads in specimens with two different bracket configurations; a full and a half bracket.

A finite element model of the specimens was made with shell elements, and the results are compared with the experimental results. There is a very good agreement in the full bracket stiffness, failure load prediction and failure location. However, for the half bracket configuration, the experimental part stiffness was lower than the FE solution.

There is a significant difference between the strains measured experimentally and the finite element strains, but the full and half brackets tested are failing at approximately the same strain level.

INTRODUCTION

Finite element analysis (FEA) is now widely used in industry as a development tool to evaluate a product's design and mechanical performance, and is particularly valuable for composite materials by managing the material anisotropy. However, many assumptions are used thorough the creation of finite element (FE) models, and it can be difficult to evaluate whether they are valid or would cause a significant error in the solution. When possible, it is a good practice to verify the results obtained numerically with mechanical testing.

In this work, the structure under study is a helicopter horizontal stabilizer slat made of carbon fiber reinforced plastic (CFRP) manufactured by resin transfer moulding (RTM). The slat is basically an airfoil with 4 integrated brackets. The structure is attached to the horizontal stabilizer with a total of 8 screws, 2 per bracket. A global FEA was conducted on the horizontal stabilizer and the slat assembly under severe aerodynamic and thermal loadings in order to optimize both part and lamina design [1]. The part manufacturability was established in previous work [2], with the construction of a prototype slat with real size cross-section airfoil and brackets, but at one third of the full-size length. To study the impact of bracket design on manufacturing, the part was

made with two different bracket designs, a full and a half bracket, as shown in Figure 1. The half bracket location is at one end of the airfoil, with its plies blending to the airfoil in one ply drop-off. In opposition, the full bracket is in a middle slat configuration with its plies blending in two ply drop-offs.

Full-size slat with full brackets

Full-size slat with half brackets

Prototype slat (half & full brackets)

Figure 1: Full-size and prototype slats with different bracket configurations

Since a few prototype slats were made available, static mechanical testing was conducted to establish the mechanical performance of the two different bracket configurations. A test fixture was developed to introduce realistic loads in the shorter slat structure for full and half brackets. Along with the test fixture, a FE model was developed to assess the part mechanical performance, and the results are compared.

1. STATIC MECHANICAL TESTING OF THE PROTOTYPE SLATS

On the full-size slat, stresses are caused by aerodynamic loading, thermal expansion and displacement of the 4 brackets that follow the motion of the horizontal stabilizer. The slat design is not optimized to provide high stiffness but to be flexible, in order to follow the displacements of the horizontal stabilizer, without sustaining damage.

Mechanical testing objectives:

- Comparison between the full and half bracket configuration with a realistic loading
- Comparison with the FEA in terms of structure stiffness, strain and failure location

To provide a realistic loading for the mechanical testing is a challenging task. Firstly, the complex combination of loads introduced on the full-size slat finite element model in [1] is difficult to simplify without losing accuracy in the stress distribution. Secondly, the prototype slat geometry is only a third of the full-size length, and the full and half brackets have different geometries and location on the airfoil.

There are many possible methods to achieve those objectives; each with advantages and disadvantages. A preferred comparison method is described below.

1.1 Comparison between the full and half brackets

It is desirable to use the same bracket location and geometry to compare the mechanical performance of full and half brackets on the slat structure. For this reason, only the middle slat location for the bracket is compared. Since there is no half bracket molded

in a middle configuration on the prototype slat, a half bracket equivalent to the full bracket is obtained by simply trimming the full bracket to remove one flange, as shown in Figure 2. The specimen airfoil left end to right end distance is 15 cm.

Figure 2: Prototype slats trimmed to obtain full and half bracket specimens in a middle configuration

1.2 Load introduction

Two different FE models were used to establish a realistic load introduction in the test specimens. The full-size slat FE model coupled with the horizontal stabilizer (from [1]) was used to determine the slat stress distribution to reproduce, and to extract the loads transferred by the fasteners. These loads were introduced in a second FE model of the specimen illustrated in Figure 2, to study the impact of load introduction on the specimen stress distribution. The specimen is fixed on both airfoil ends and the loads are applied via the fasteners. To make this loading experimentally viable, only the vertical forces (z-direction in Figure 3) were kept. Even though the resultant loading is very simplified, it does reproduce a realistic stress distribution on both full and half bracket specimens.

It is important to notice that on the full-size slat, the loads transferred by the fasteners on a full bracket configuration are different that those of a half bracket configuration, due to the change in slat stiffness. However, the same loading is applied experimentally on both full and half bracket specimens for comparison purposes.

1.3 Test fixture design

The test fixture is designed to be used on a 5 kN MTS Insight™ electromechanical test system. As described above, the specimen is fixed on both airfoil ends. As illustrated in Figure 3, the rear fastener is located at a distance *c* from the front fastener. To induce the desired forces at the fastener locations, the force *F* is applied at a distance *b* from the front fastener.

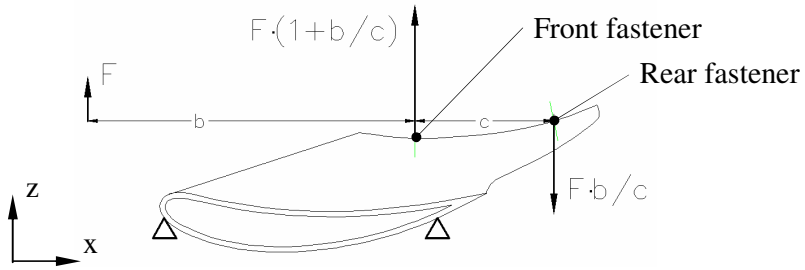

Figure 3: Specimen side view with the load application vectors

The test fixture is shown on Figure 4. The assembly is as follow. The specimen is fixed to the base by the four airfoil corners. The specimen bracket is then screwed to a machined block representing the horizontal stabilizer. The block is linking the specimen bracket to the MTS test frame through a fixture with bearings sliding in slotted holes. The slotted holes are allowing displacement in the x-direction, therefore making sure that only loads in the z-direction are introduced in the specimen. To test the half bracket in the same conditions as the full bracket, guides were used to prevent the half bracket from tilting, making sure that all displacements would be in the z-direction. For stiffness reasons, all fixture components are made of steel.

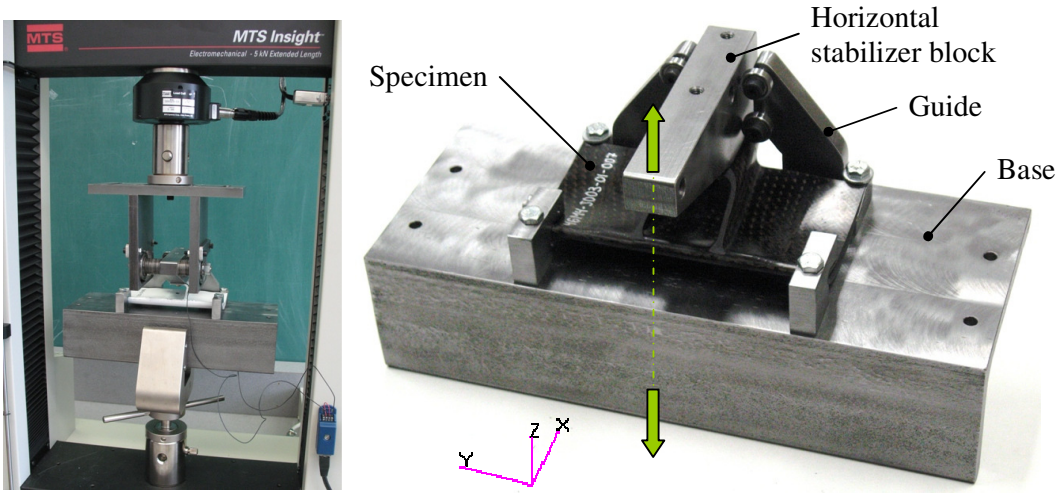

Figure 4: Test fixture

1.4 Experimental procedure

Two full bracket and two half bracket specimens were tested to destruction. To prevent the airfoil from buckling in the areas where the airfoil is fixed to the fixture, the airfoil was filled with epoxy resin over 1.5 cm at both ends. The specimens were instrumented with a 9.5 mm strain gage on the upper bracket radius to compare the strain with the finite element results. These relatively long strain gages were chosen to minimize the variability in strain measurement for inhomogeneous materials with a large unit cell size [3]. The unit cell size for the 5 harness satin carbon fabric used in the prototype fabrication is approximately 11.5 mm. The parts were then painted in white to facilitate visual inspection of crack formation during the tests. The tests were controlled in displacement at a rate of 0.5 mm/min, with load and strain acquisition.

2. FINITE ELEMENT MODEL

A finite element model with full and half bracket specimens was created in *Patran* with the *Laminate Modeler* module. The *Laminate Modeler* module is simulating the draping process and is used to generate the corresponding laminate material properties. *MD Nastran* is used as the solver.

The prototype slat airfoil and brackets are made of 5 and 6 layers of bi-directional CFRP respectively. The lay-up sequence is $[45]_5$ on the airfoil and $[45/0/45]_s$ on the bracket, while the ply drop-off is as shown in Figure 5.

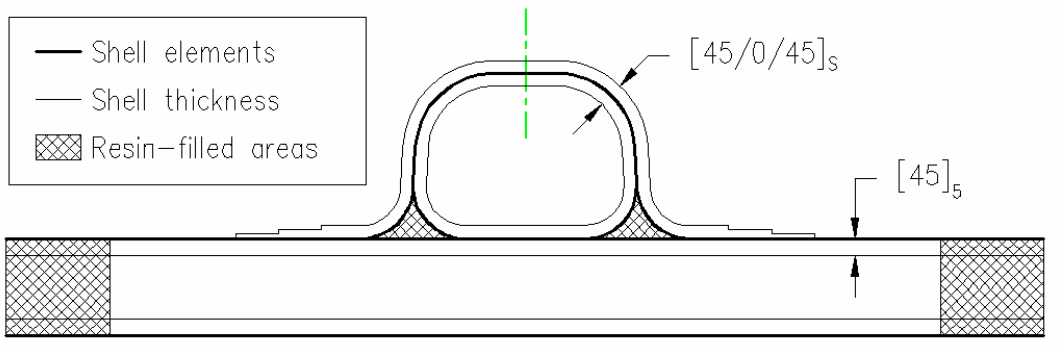

Figure 5: Cross-section view of the prototype slat airfoil and bracket lay-up

The specimen was modeled with Quad4 shell elements. The regions filled with resin are made of 3D Hex8 or tetrahedral Tet4 elements. The typical element edge length is 0.75 mm.

To model the test fixture boundary conditions, the FE model displacements were fixed in the regions where contact is made between the fixture and the slat airfoil. Assuming a high rigidity in the fixture where the load is applied, a rigid body element is used to transfer the load to the fasteners. The fasteners are modeled with 1D bush, RBE3 and Quad4 shell elements. These shell elements are the size of the screw head with steel material properties and a thickness of 2.5 mm.

The mechanical properties used for the composite are those of CYCOM® 890 RTM / AS4-GP 6K-5HS woven carbon fabric. Most values were available from the technical data sheet, except for the Poisson's ratio υ_{12} taken from [1]. In the areas filled with resin (such as the airfoil tips and bracket radius), the material properties used are those of the neat resin CYCOM® 890 RTM, presented in Table 1. The failure criterion used is Tsai-Wu, with an interaction term of -0.5.

Table 1: Mechanical properties of constituent materials

Material	Linear elastic material properties		Strength material properties	
890RTM / AS4-GP-6K-5HS (orthotropic)	E_{11} (GPa)	64	$S_{11}^{(+)}$ (MPa)	886
	E_{22} (GPa)	60	$S_{22}^{(+)}$ (MPa)	755
	E_{12} (GPa)	4.3	$S_{11}^{(-)}$ (MPa)	713
	E_{23} (GPa)	1.3	$S_{22}^{(-)}$ (MPa)	708
	E_{13} (GPa)	1.3	S_{12} (MPa)	97
	υ_{12}	0.04	S_{13} (MPa)	76
			S_{23} (MPa)	76
890RTM neat resin (isotropic)	E (GPa)	3.1	$S_{11}^{(+)}$ (MPa)	70
	G (GPa)	1.3		
	υ	0.19		

3. EXPERIMENTAL AND FEA RESULTS

Since the FE solver used provides a static linear elastic solution, it does not consider fracture mechanics. Therefore, the model is not valid beyond the first part damage, where the structure stiffness is typically reducing with the increase of damage.

Given a certain failure criterion, the FEA failure prediction can be compared with the experimental results. For this reason, it is important to experimentally detect the first failure to occur in the specimen. The first damage was determined jointly by three methods; a drop in the load vs. displacement curve, the noise when the specimen is cracking and by visual inspection. During the mechanical testing, it was observed that the first damage could not be seen visually, and that only the increase of displacement would eventually generate the first visible damage.

The front view in Figure 6 shows the first visible damage observed in the specimen half bracket mechanical testing. When the test was resumed after the first visible damage, a failure could then be observed from the rear view on the bracket trailing edge, in compression. Furthermore, a slight crack appeared from the front fastener region, heading towards the bracket trailing edge failure. The failure location (i.e. first visible damage) on the full bracket specimens was the same as observed in the half bracket specimens.

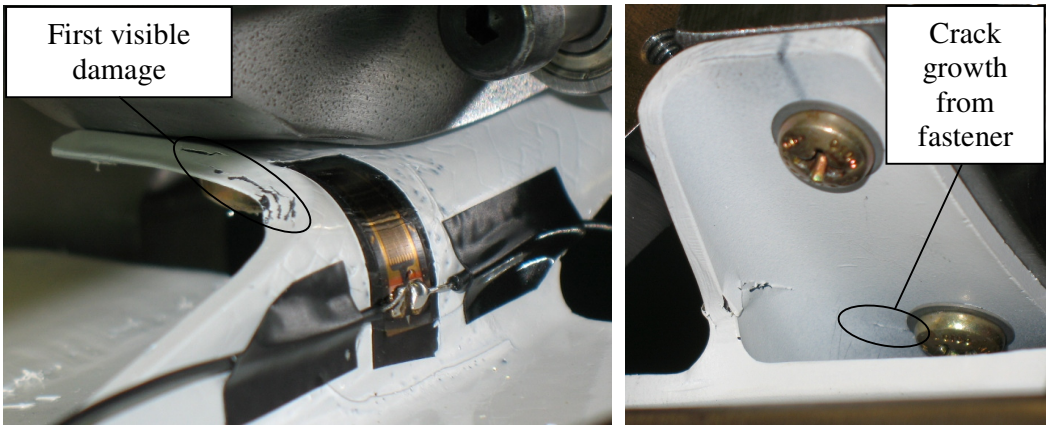

Figure 6: Visible damage on half bracket specimen, front and rear view

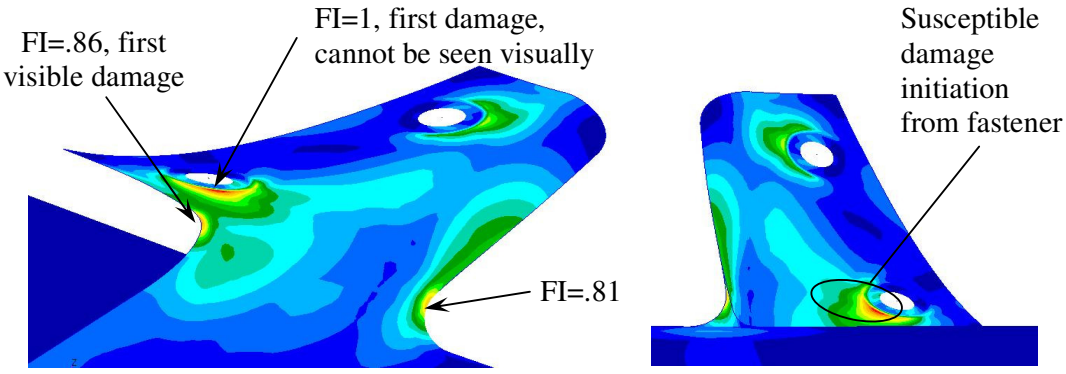

Figure 7: Tsai-Wu failure index distribution, front and rear view

From a qualitative point of view, it is interesting to compare the failure locations observed experimentally with the failure index distribution given by the Tsai-Wu failure criterion, illustrated in Figure 7. The higher failure index is observed next to the front hole, where the front screw creates a stress concentration in the lamina. The next higher failure index is located in the front bracket radius, where the first visual damage is observed on the specimens. Then, the third failure index in order of importance is located at the bracket trailing edge, close to the airfoil, which corresponds with the experimental results. The location of the first nonvisible damage still remains unknown. However, if the stress concentration around the front fastener is real (not caused by an inadequate load introduction in the FE model), then the first nonvisible damage might be in the front fastener region, and eventually growing to form a crack oriented towards the bracket trailing edge existing damage.

The Figure 8 presents the experimental and FE loads with respect to the test frame displacement, including the first nonvisible and visible damage. In the FE results, the first location to reach a failure index of 1 (first part damage) is in the fastener area and considered nonvisible. Beyond this point, the FE model is not valid because it should locally decrease the material properties according to the failure, resulting in reduced structure stiffness. However, if we still increase the displacement (with over-estimated structure stiffness), the next location to reach a failure index of 1 is in the bracket front radius, and is considered as the first visible damage.

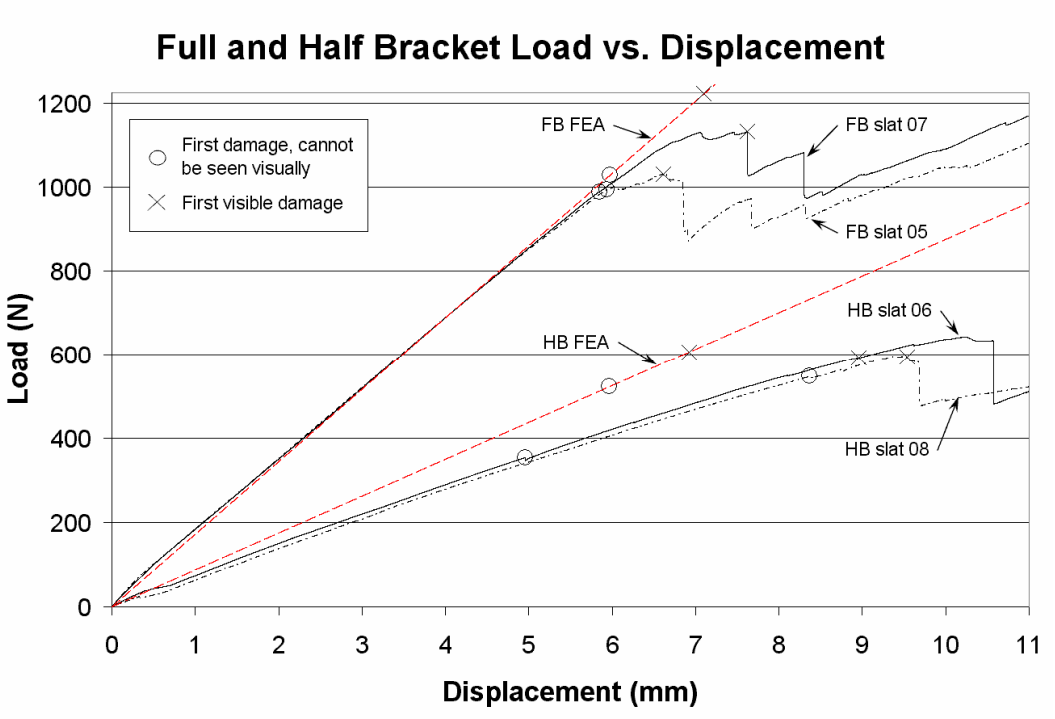

Figure 8: Load vs. displacement curves for 2 full and 2 half bracket configurations

There is good agreement between the experimental and FE full bracket stiffness. Moreover, the first failure is very close to the first nonvisible damage for both slat 05 and 07. Beyond that point, even though there is no stiffness degradation in the FE

model, the FE model displacement at the first visible damage is within the experimental range.

However, the experimental stiffness of the half bracket specimens is lower than the stiffness obtained with the FEA. In opposition to the full bracket symmetry, the half bracket geometry induces lateral and torsion reaction forces in the fixture. The lower stiffness observed in the experimental results may be related to the fixture lack of lateral and torsional stiffnesses. It would also provide an explanation for the slight non-linearity in the load/displacement curve for both half bracket tests. The early damage detected in specimen 06 is probably attributable to the high void content in the part, which was observed before testing.

The strain gage readings are plotted in Figure 9 along with the FEA strain. The FEA strain was extracted from the outer layer, by averaging the strain of the corresponding elements in the strain gage orientation. While the FEA is predicting similar strain for both full and half brackets with respect to the displacement, a higher and different strain rate is observed in the experimental results for the two bracket configurations. In the FE model, there is a large variation in the strain over the strain gage area. The large strain gage size installed in a region of non-uniform strains may have contributed to the differences in strain. However, it is interesting to note that the four test parts show the first visible signs of damage at a strain of approximately 0.008 mm/mm.

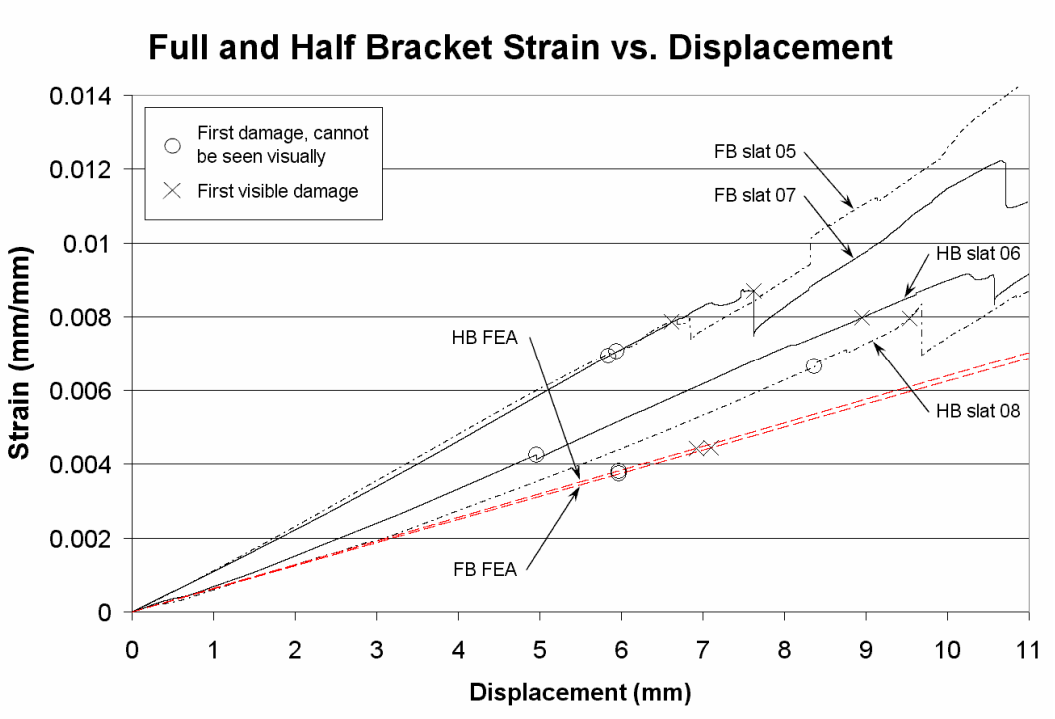

Figure 9: Strain vs. displacement curves for 2 full and 2 half bracket specimens

CONCLUSION

The test fixture successfully introduced a realistic loading in the prototype slat specimens for both full and half bracket configurations. The boundary conditions used on the specimens were suitable to avoid any local damage to the structure. Considering the fact that only two specimens were tested for each bracket configuration and that these parts were made during the development of the manufacturing process, the consistency in the mechanical testing results is noteworthy.

A very good agreement between the experimental and numerical results of the full bracket stiffness was obtained. However, the stiffness differences observed for the half bracket would require further attention. In addition, the strains extracted from the FE results did not match those acquired experimentally with the strain gages. The large strain gage size in an area of high strain gradient might have contributed to these differences.

The failure prediction by using the Tsai-Wu failure criterion provided a good estimation of the load to failure and failure location. Since most of the failures observed were interlaminar, the use of a 3D solid element model would also provide the out-of-plane stresses that could lead to a better understanding of the interlaminar damage initiation.

The data acquired in the scope of this work will facilitate the comparison between the full and half bracket configurations and the design of the next composite slat structures.

ACKNOWLEDGEMENTS

The authors would like to acknowledge the technical contribution of Peter Minderhoud and Simon Bernier, BHTCL, for their support in the FEA and the elaboration of the test fixture. This work is carried out as part of CRIAQ Project 1.15: Optimized Design of Composite Parts by RTM. Support for this project is provided by Bell Helicopter Textron Canada Limited (BHTCL), the National Research Council of Canada (Aerospace Manufacturing Technology Centre, Institute for Aerospace Research), Delastek Inc., McGill University, École Polytechnique de Montréal, the Natural Sciences and Engineering Research Council of Canada (NSERC), and the Consortium for Research and Innovation in Aerospace in Quebec (CRIAQ).

REFERENCES

1. Thériault, F., *Optimized design of a composite helicopter structure by resin transfer moulding*, in *Department of Mechanical Engineering*. 2007, McGill University: Montreal. p. 150.
2. O'Flynn, J., *Design for manufacturability of a composite helicopter structure made by resin transfer moulding*, in *Department of Mechanical Engineering*. 2007, McGill University: Montreal. p. 81.
3. Masters, J.E., *Strain Gage Selection Criteria for Textile Composite Materials*, in *NASA Contractor Report 198286*. 1996, Lockheed Martin Engineering and Sciences Company.